

## Electrochemically Triggered Double Translocation of Two Different Metal Ions with a Ditopic Calix[6]arene Ligand

Benoit Colasson,<sup>†</sup> Nicolas Le Poul,<sup>‡</sup> Yves Le Mest,<sup>\*,‡</sup> and Olivia Reinaud<sup>\*,†</sup>

*Laboratoire de Chimie et Biochimie Pharmacologiques et Toxicologiques, CNRS, UMR 8601, Université Paris Descartes, 45 rue des Saints Pères, 75006 Paris, France and Laboratoire de Chimie, Electrochimie Moléculaires et Chimie Analytique, CNRS, UMR 6521, Université Européenne de Bretagne à Brest, CS 93837, 6 Avenue Le Gorgeu, 29238 Brest Cedex 3, France*

Received December 18, 2009; E-mail: olivia.reinaud@parisdescartes.fr; yves.lelest@univ-brest.fr

**Abstract:** A ditopic ligand based on a calix[6]arene with three imidazoles (Im) appended at the small rim and three triazoles (Tria) at the large one is able to form selectively two stable heterodinuclear complexes with  $Zn^{II}/Cu^{I/Tria}$  and  $Cu^{II}/Zn^{II/Tria}$ . In the  $Cu^I$  case, the zinc cation is preferentially coordinated at the Im site while the copper is bound at the Tria site. The situation is the opposite when  $Cu^{II}$  is used. The position of the two cations within the complex can be electrochemically switched via the oxidation–reduction of the copper cation between oxidation states +I and +II. The presence of the zinc cation is crucial (i) to control the bistability of the system by an allosteric structuring role and (ii) to promote the metal switch since the monocopper complex exhibits reversible behavior with Cu located at the imidazole site in both oxidation states. This represents the first example of a double translocation of two different metal cations.

### Introduction

For the past decade, we have been involved in the mimicking of the active site of mononuclear metalloenzymes. We have been using the calix[6]arene macrocycle to isolate the metal center, prevent dimerization, and hence play the role of the enzymatic pocket. In this system, the hydrophobic cavity of the calixarene core provides secondary interactions between the host (the calix complex) and a guest (an exogenous ligand).<sup>1</sup> More recently, we have been interested in developing systems that can bind two metal centers at a controlled distance, higher than 4 Å, in order to escape the thermodynamic sink leading to the formation of bridged and electronically coupled dinuclear complexes.<sup>2</sup> Indeed, many enzymes involve two metal ions displaying different functions,<sup>3,4</sup> which raises interesting questions relative to the selective binding of two different metal ions at two different sites: mutual structural roles, selective metal ion loading and trafficking, and thus translocation processes.<sup>5</sup> These considerations led us to investigate the selective binding of two

different metal ions within the heteroditopic ligand **1** (Figure 1).<sup>2b</sup> The small rim of this calix[6]arene is functionalized with three imidazole (Im) arms, whereas the large rim is decorated with three 1,4-disubstituted-1,2,3-triazole (Tria) units formed during the  $Cu^I$ -catalyzed cycloaddition between the trisazido calixarene and three acetylenes.<sup>6</sup> We have shown that this ligand can bind two  $Zn^{II}$  ions that are isolated from each other. Interestingly, the first equivalent of  $Zn^{II}$  binds very selectively the Im site, which induces the preorganization of the calixarene large rim for the coordination of a second  $Zn^{II}$  cation at the Tria site in an allosterically constrained trigonal environment.<sup>2b</sup> The capability of this ligand to bind selectively 1 or 2 equiv of  $Zn^{II}$  indicates a large difference between the two coordinating sites [ $K_a^{Tria}(Zn) = 3 \times 10^5$  whereas  $K_a^{Im}(Zn) > 10^8$  in  $CH_3CN$ ]. Thus, the ditopic ligand **1** appeared to be a good candidate in order to study the selective coordination toward two different metal cations, one of which is redox active. Indeed, while the Im site can accommodate a metal center in a trigonal or tetragonal geometry, the Tria binding site seems to be much less flexible. We anticipated that the difference in the geometric requirements of  $Cu^{II}$  and  $Cu^I$  cations might tune the binding mode of the ligand. The combination of the selective coordination of the cation pairs  $Zn^{II}/Cu^I$  and  $Zn^{II}/Cu^{II}$  associated with the lability of the binding sites might provide a new entry for translocation processes.

<sup>†</sup> Université Paris Descartes.

<sup>‡</sup> Université Européenne de Bretagne à Brest.

- (1) (a) Coquièrre, D.; Le Gac, S.; Darbost, U.; Sénèque, O.; Jabin, I.; Reinaud, O. *Org. Biomol. Chem.* **2009**, *7*, 2485–2500. (b) Le Poul, N.; Douziech, B.; Zeitouny, J.; Thiabaud, G.; Colas, H.; Conan, F.; Cosquer, N.; Jabin, I.; Lagrost, C.; Hapiot, P.; Reinaud, O.; Le Mest, Y. *J. Am. Chem. Soc.* **2009**, *131*, 17800–17807. (c) Le Poul, N.; Campion, M.; Izzet, G.; Douziech, B.; Reinaud, O.; Le Mest, Y. *J. Am. Chem. Soc.* **2005**, *127*, 5280–5281. (d) Izzet, G.; Zeitouny, J.; Akdas-Killig, H.; Frapart, Y.; Ménage, S.; Douziech, B.; Jabin, I.; Le Mest, Y.; Reinaud, O. *J. Am. Chem. Soc.* **2008**, *130*, 9514–9523. (e) Thiabaud, G.; Guillemot, G.; Schmitz-Afonso, I.; Colasson, B.; Reinaud, O. *Angew. Chem., Int. Ed.* **2009**, *48*, 7383–7386.
- (2) (a) Coquièrre, D.; Marrot, J.; Reinaud, O. *Chem. Commun.* **2006**, 3924–3926. (b) Colasson, B.; Save, M.; Milko, P.; Roithová, J.; Schröder, D.; Reinaud, O. *Org. Lett.* **2007**, *9*, 4987–4990.
- (3) In copper mono-oxygenases, for example, one metal center activates  $O_2$  whereas the second one handles the sequential input of two electrons. Klinman, J. P. *J. Biol. Chem.* **2006**, *281*, 3013–3016.

- (4) In the copper–zinc superoxide dismutase enzyme, the Cu site catalyzes the disproportionation of the superoxide free radical whereas the Zn site has a crucial structural role. In that case, it is quite remarkable that the redox-active copper cation, which changes its oxidation state during the catalytic cycle, remains bound in the same environment. Tainer, J. A.; Getzoff, E. D.; Beem, K. M.; Richardson, J. S.; Richardson, D. C. *J. Mol. Biol.* **1982**, *160*, 181–217.
- (5) Boal, A. K.; Rosenzweig, A. C. *Chem. Rev.* **2009**, *109*, 4760–4779.
- (6) (a) Tormøe, C. W.; Christensen, C.; Meldal, M. *J. Org. Chem.* **2002**, *67*, 3057–3062. (b) Rostovtsev, V. V.; Green, L. G.; Fokin, V. V.; Sharpless, K. B. *Angew. Chem., Int. Ed.* **2002**, *41*, 2596–2599.

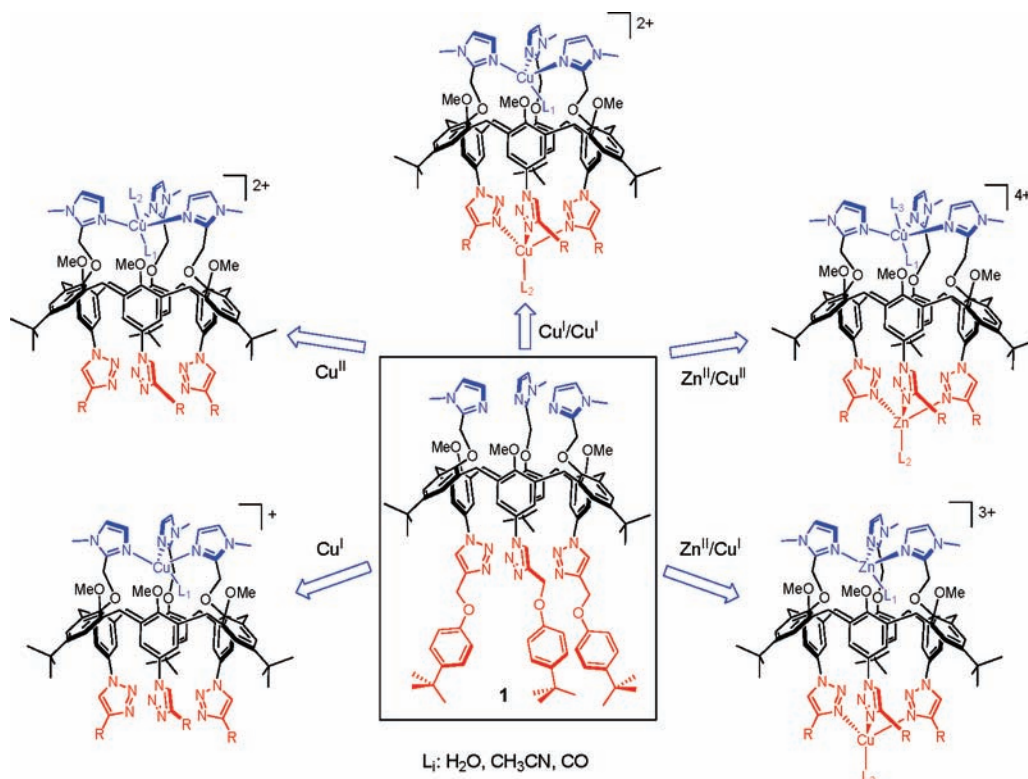


**Figure 1.** Structural representation of ligand **1** and related complexes studied in this work.

So far, few synthetic systems capable of translocation have been studied.<sup>7</sup> Most of them are based on the translocation of only one particle (either a cation or an anion).<sup>8</sup> Fabbrizzi and co-workers described the only example of a double translocation of two Cu<sup>II</sup> cations in a macrocyclic molecule in response to an acid–base stimulus coupled with host recognition.<sup>9</sup> In this system, the macrocycle presents two pairs of identical binding sites for the two Cu<sup>II</sup> ions which, in both situations, are located in the same environment and therefore play the same role.

Herein, we report the first example of a double translocation of one zinc cation and one copper cation. The translocation takes place between two different binding sites appended at the two opposite rims of a calix[6]arene. The driving force of the process is the electrochemical switch of the copper cation between its oxidation states I and II coupled with the balance between the preferential coordinating mode of the ditopic ligand **1** for the two pairs of cations Zn<sup>II</sup>/Cu<sup>I</sup> and Zn<sup>II</sup>/Cu<sup>II</sup>.

## Results and Discussion

**Mono- and Bis-Cu Complexes: Synthesis and Characterization. Mono-Cu<sup>I</sup> and Mono-Cu<sup>II</sup>.** The monometallic Cu<sup>I</sup> and Cu<sup>II</sup> complexes were synthesized in THF by mixing, in equimolar amounts (1:1), ligand **1** with [Cu(CH<sub>3</sub>CN)<sub>4</sub>](PF<sub>6</sub>) and [Cu(H<sub>2</sub>O)<sub>6</sub>](ClO<sub>4</sub>)<sub>2</sub>, respectively. By comparison with

**Table 1.** Spectroscopic (Vis<sup>a</sup> EPR<sup>b</sup>) and Electrochemical Data<sup>c</sup> for Mono-Cu-**1**, Bis-Cu-**1**, and Zn/Cu-**1** Complexes at Both Cu<sup>I</sup> and Cu<sup>II</sup> Redox States (L = CH<sub>3</sub>CN, H<sub>2</sub>O)

|   | $\lambda_{\text{max}}/\text{nm}$<br>( $\epsilon/\text{M}^{-1} \text{cm}^{-1}$ ) | $g$ value (A/G)                                     | $E_{1/2}/\text{V}$ ( $\Delta E_p/\text{mV}$ ) <sup>d</sup>  |
|---|---|---|---|
| [Cu <sup>II</sup> (Im <sub>3</sub> calix[6]arene)(L) <sub>2</sub> ] <sup>2+</sup> <sup>e</sup>                | 758 (34)  | $g_{\parallel} = 2.31$ (135),<br>$g_{\perp} = 2.06$ | 0.06 (400)  |
| [Cu <sup>I</sup> <sub>im</sub> ( <b>1</b> )(L)] <sup>+</sup>  |   |   | 0.05 (150)  |
| [Cu <sup>II</sup> <sub>im</sub> ( <b>1</b> )(L) <sub>2</sub> ] <sup>2+</sup>                                  | 757 (82)  | $g_{\parallel} = 2.30$ (147),<br>$g_{\perp} = 2.06$ | 0.05 (120)  |
| [Cu <sup>I</sup> <sub>im</sub> Cu <sup>I</sup> <sub>tria</sub> ( <b>1</b> )(L) <sub>2</sub> ] <sup>2+</sup>   |   |   | 0.05 (95), 0.70 (170)   |
| [Zn <sup>II</sup> <sub>im</sub> Cu <sup>I</sup> <sub>tria</sub> ( <b>1</b> )(L) <sub>2</sub> ] <sup>3+</sup>  |   |   | $E_{\text{pa}} = 0.75^f$ ( $E_{\text{pc}} = 0.01$ ) <sup>f,s</sup><br>[0.05 (80)] <sup>h,i</sup> 0.70 (80) <sup>h</sup> |
| [Cu <sup>II</sup> <sub>im</sub> Zn <sup>II</sup> <sub>tria</sub> ( <b>1</b> )(L) <sub>3</sub> ] <sup>4+</sup> | 759 (94)  | $g_{\parallel} = 2.30$ (155),<br>$g_{\perp} = 2.07$ | $E_{\text{pc}} = 0.01^f$ ( $E_{\text{pa}} = 0.70$ ) <sup>f,s</sup>  |

<sup>a</sup> In CH<sub>3</sub>CN. <sup>b</sup> In frozen 0.1 M CH<sub>3</sub>CN/NBu<sub>4</sub>ClO<sub>4</sub>. <sup>c</sup> In 0.1 M CH<sub>3</sub>CN/NBu<sub>4</sub>ClO<sub>4</sub>, Pt WE; E/V vs Fc;  $\Delta E_p$  at 0.1 V s<sup>-1</sup>. <sup>d</sup> For reversible processes. <sup>e</sup> From ref. 12. <sup>f</sup> Irreversible peak in concentrated solution (2 mM). <sup>g</sup> Irreversible peak detected on the reverse scan. <sup>h</sup> Reversible process in diluted solution (0.1 mM). <sup>i</sup> Electrochemically generated at low potential.

the previously studied [Cu<sup>I</sup>(Im<sub>3</sub>calix[6]arene)(L)]<sup>+</sup><sup>10</sup> and [Cu<sup>II</sup>(Im<sub>3</sub>calix[6]arene)(L)<sub>2</sub>]<sup>2+</sup>,<sup>11</sup> having *tert*-butyl groups instead of triazolyl groups at the large rim, the spectroscopic data (Table 1) indicate that the metal is located at the Im site, preferentially to the Tria site, in both redox states, leading to [Cu<sup>I</sup><sub>im</sub>(**1**)]<sup>+</sup> and [Cu<sup>II</sup><sub>im</sub>(**1**)(L)<sub>2</sub>]<sup>2+</sup> (L = H<sub>2</sub>O or CH<sub>3</sub>CN) (Figure 1). The tetrahedral environment around the Cu<sup>I</sup> center was best evidenced through its CO adduct, [Cu<sup>I</sup><sub>im</sub>(**1**)(CO)]<sup>+</sup>, readily obtained after CO bubbling in a noncoordinating solvent. Indeed, the

(7) Amendola, V.; Fabbrizzi, L.; Mangano, C.; Pallavicini, P. *Acc. Chem. Res.* **2001**, *34*, 488–493.

(8) (a) Zelikovitch, L.; Libman, J.; Shanzer, A. *Nature* **1995**, *374*, 790–792. (b) Belle, C.; Pierre, J.-L.; Saint Aman, E. *New J. Chem.* **1998**, *139*, 9–1402. (c) Kalny, D.; Elhabiri, M.; Moav, T.; Vaskevich, A.; Rubinstein, I.; Shanzer, A.; Albrecht-Gart, A.-M. *Chem. Commun.* **2002**, 1426–1427. (d) Amendola, V.; Colasson, B.; Fabbrizzi, L.; Rodriguez Douton, M.-J. *Chem.–Eur. J.* **2007**, *13*, 4988–4997.

(9) Fabbrizzi, L.; Foti, F.; Patroni, S.; Pallavicini, P.; Taglietti, A. *Angew. Chem., Int. Ed.* **2004**, *43*, 5073–5077.

(10) Rondelez, Y.; Sénèque, O.; Rager, M.-N.; Duprat, A. F.; Reinaud, O. *Chem.–Eur. J.* **2000**, *6*, 4218–4226. (b) Rondelez, Y.; Bertho, G.; Reinaud, O. *Angew. Chem., Int. Ed.* **2002**, *41*, 1044–1046.

(11) (a) Le Clainche, L.; Giorgi, M.; Reinaud, O. *Inorg. Chem.* **2000**, *39*, 3436–3437. (b) Le Clainche, L.; Rondelez, Y.; Sénèque, O.; Blanchard, S.; Campion, M.; Giorgi, M.; Duprat, A. F.; Le Mest, Y.; Reinaud, O. *C. R. Acad. Sci., Chim., Ser. IIc* **2000**, *3*, 811–819.

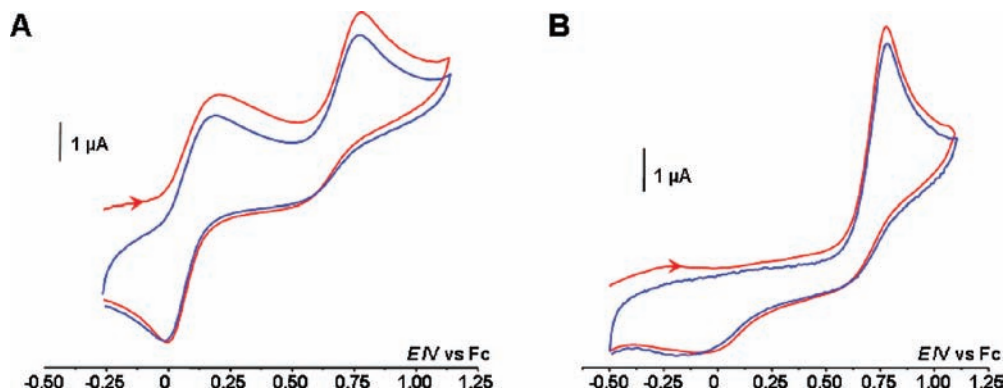


**Figure 2.** Cyclic voltammogram at a Pt electrode in 0.1 M CH<sub>3</sub>CN/NBu<sub>4</sub>ClO<sub>4</sub> [1st (red) and 2nd (blue) cycles] of (A) [Cu<sup>I</sup><sub>Im</sub>Cu<sup>I</sup><sub>Tria</sub>(1)(L)<sub>2</sub>]<sup>2+</sup> and (B) [Zn<sup>II</sup><sub>Im</sub>Cu<sup>I</sup><sub>Tria</sub>(1)(L)<sub>2</sub>]<sup>3+</sup> (L = CH<sub>3</sub>CN, H<sub>2</sub>O). Concentration = 2 mM; E/V vs Fc;  $\nu = 0.1 \text{ V s}^{-1}$ .

sharp <sup>1</sup>H NMR signature (Figure S1, Supporting Information) attested to the C<sub>3v</sub> symmetry of the complex due to the coordination of all three imidazole arms and one CO guest ( $\nu_{\text{CO}} = 2100 \text{ cm}^{-1}$ ), as previously described for the parent compound.<sup>10</sup> For the cupric complex as well, the spectroscopic data (UV-vis and EPR, see Table 1 and Figures S11–S15, Supporting Information) are quite similar to those of the parent compounds,<sup>11</sup> indicating a tetragonal environment with two exogenous ligands, one in the endo and the other in the exo position. All of these statements are confirmed by the voltammetric data ( $E_{1/2} = 0.05 \text{ V vs Fc}^+/\text{Fc}$ ) in 0.1 M CH<sub>3</sub>CN/NBu<sub>4</sub>ClO<sub>4</sub> (Table 1 and Figure S16, Supporting Information), which are nearly identical to that previously obtained for the monometallic parent complex, [Cu<sup>III</sup>(Im<sub>3</sub>calix[6]arene)(L)]<sup>2+/+</sup>, bearing a trisimidazole cap but no triazole ( $E_{1/2} = 0.06 \text{ V}$ ).<sup>12</sup> Interestingly, the large decrease in peak separation, in comparison to [Cu<sup>I</sup>(Im<sub>3</sub>calix[6]arene)(L)]<sup>+</sup> ( $\Delta E_p = 150 \text{ vs } 400 \text{ mV}$ ), highlights a faster redox process ascribed to a decrease of the reorganizational energy associated to the Cu<sup>II</sup> vs Cu<sup>I</sup> coordination change. This is probably induced by the lower flexibility of the whole structure due to the presence of triazole groups, as already observed for hindered Cu(RIm<sub>3</sub>R'calix[6]arene) complexes (where R and R' are adaptable alkyl-substituting groups on the large rim of the calixarene and on the imidazole rings, respectively).<sup>12a</sup>

**Cu<sup>I</sup>/Cu<sup>I</sup>.** Addition of a second cuprous ion to the monometallic [Cu<sup>I</sup><sub>Im</sub>(1)(CH<sub>3</sub>CN)](PF<sub>6</sub>) yields the bimetallic complex: [Cu<sup>I</sup><sub>Im</sub>Cu<sup>I</sup><sub>Tria</sub>(1)(CH<sub>3</sub>CN)<sub>2</sub>](PF<sub>6</sub>)<sub>2</sub>. <sup>1</sup>H NMR spectroscopy clearly supports the presence of one Cu<sup>I</sup> at the Tria site since a sharp peak emerges at 7.33 ppm in CDCl<sub>3</sub> saturated with CO (Figure S2, Supporting Information). Oxidation of the bimetallic compound was investigated by cyclic voltammetry (CV) (Figures 2A and S17, Supporting Information) (Table 1). The Cu<sup>I</sup><sub>Im</sub> is oxidized reversibly at  $E_{1/2} = 0.05 \text{ V}$  at the same potential as the mono-Cu<sup>I</sup> complex. The second oxidation (Cu<sup>I</sup><sub>Tria</sub>) occurs at  $E_{1/2} = 0.70 \text{ V}$  with a broad reverse cathodic peak. The highly positive value of the redox potential obtained for the Cu triazole system is indicative of stabilized Cu<sup>I</sup> and destabilized Cu<sup>II</sup> species. Both effects, electronic (weak donor effect of the triazole vs imidazole) and geometric (strong preference for a tetrahedral

geometry around the metal center forced by the rigid disposition of the triazoles at the large rim of the calixarene macrocycle), are likely combined to result in such a potential value. Quantitative electrolysis ( $n = 1 \text{ e}^-$ ) at a potential intermediate between both systems ( $E = 0.20 \text{ V}$ ) allowed the selective formation of a stable mixed valence complex [Cu<sup>II</sup><sub>Im</sub>Cu<sup>I</sup><sub>Tria</sub>] (Figure S18, Supporting Information). Further electrolysis at  $E = 0.80 \text{ V}$  leads to an unstable bis-cupric species [Cu<sup>II</sup><sub>Im</sub>Cu<sup>II</sup><sub>Tria</sub>], in agreement with the weak reversibility of the Cu<sup>III</sup><sub>Tria</sub> system on the CV time scale ( $0.02 < \nu < 10 \text{ V s}^{-1}$ ).<sup>13</sup>

**Zn<sup>II</sup>/Cu<sup>III</sup> Complexes: Double Translocation Effect under a Redox Stimulus.** These preliminary experiments have shown that (i) the Im versus Tria environment of the copper ion could be clearly identified by electrochemistry and <sup>1</sup>H NMR spectroscopy, (ii) Cu<sup>I</sup> and Cu<sup>II</sup> are preferentially located at the Im versus Tria site in the mononuclear complexes, and (iii) the Tria site is suitable for one Cu<sup>I</sup> but does not fulfill the geometric requirements for the stabilization of a single Cu<sup>II</sup> cation. We thus pursued this study by investigating the effect of the substitution of one Cu<sup>III</sup> by a Zn<sup>II</sup> and the influence of the redox state of Cu (+I or +II) on the structural, spectroscopic, and electrochemical properties of the resulting new complexes.

**Zn<sup>II</sup>/Cu<sup>I</sup>.** Synthesis of the Zn<sup>II</sup>/Cu<sup>I</sup> complex was performed by adding [Cu(CH<sub>3</sub>CN)<sub>4</sub>](PF<sub>6</sub>) to the [Zn<sup>II</sup><sub>Im</sub>(1)(L)]<sup>2+</sup> complex. The titration, monitored by <sup>1</sup>H NMR in CD<sub>3</sub>CN, indicated that Cu<sup>+</sup> binds the Tria site to yield [Zn<sup>II</sup><sub>Im</sub>Cu<sup>I</sup><sub>Tria</sub>(1)(CD<sub>3</sub>CN)<sub>2</sub>](PF<sub>6</sub>)(ClO<sub>4</sub>)<sub>2</sub>. Indeed, the resonance of the protons attached to the triazole rings (H<sub>triaz</sub>) undergoes a characteristic downfield shift (Figure 3). The equilibrium constant was estimated to be  $K_a^{\text{Tria}}(\text{Cu}) = 1 \times 10^4$  (Figure S4, Supporting Information). The stoichiometry of the complex [Zn<sup>II</sup><sub>Im</sub>Cu<sup>I</sup><sub>Tria</sub>(1)(CH<sub>3</sub>CN)<sub>2</sub>]<sup>3+</sup> was confirmed by electrospray-mass spectrometry with a peak at  $m/z = 663.1$  corresponding to the triply charged cation

(12) (a) Le Poul, N.; Campion, M.; Douziech, B.; Rondelez, Y.; Le Clainche, L.; Reinaud, O.; Le Mest, Y. *J. Am. Chem. Soc.* **2007**, *129*, 8801–8810. (b) The electrochemical behavior of all present complexes was briefly examined in 0.1 M CH<sub>2</sub>Cl<sub>2</sub>/NBu<sub>4</sub>ClO<sub>4</sub> and is essentially similar except that the CVs are much less well resolved due to the absence of the CH<sub>3</sub>CN preorganizing molecule (refs 1c and 12a). In addition, the translocation process is observed in CH<sub>2</sub>Cl<sub>2</sub>.

(13) To further investigate the chemical evolution of the bis-Cu<sup>II</sup> complex, we attempted to prepare the complex by adding, in THF, 2 mol equiv of Cu(OTf)<sub>2</sub> to the ligand 1. From elemental analysis, the molecular structure of the green precipitate was found to possess 3 copper centers and to be pentacationic. The EPR spectrum of this complex in frozen CH<sub>3</sub>CN, which is very similar to the spectrum of the mixed valence complex [Cu<sup>II</sup><sub>Im</sub>Cu<sup>I</sup><sub>Tria</sub>], seems to indicate that two out of the three copper centers are antiferromagnetically coupled. Also, rotating-disk electrode voltammetry (RDEV) in CH<sub>3</sub>CN shows a reduction wave at  $E_{1/2} = 0.05 \text{ V}$ , attesting to the absence of Cu<sup>II</sup> at the Tria site (Figure S19, Supporting Information). These results suggest that the unstable Cu<sup>II</sup><sub>Tria</sub> evolves toward a dinuclear bridged center, most likely a hydroxo complex, thus giving rise to [Cu<sub>2</sub>(OH)(1)(L)<sub>4</sub>]<sup>5+</sup> (UV-vis and EPR spectroscopic data in CH<sub>3</sub>CN:  $\lambda_{\text{max}} = 720 \text{ nm}$ ,  $\epsilon = 210 \text{ M}^{-1} \cdot \text{cm}^{-1}$ ;  $g_{\parallel} = 2.29$  ( $A = 152 \text{ G}$ ),  $g_{\perp} = 2.06$ ).

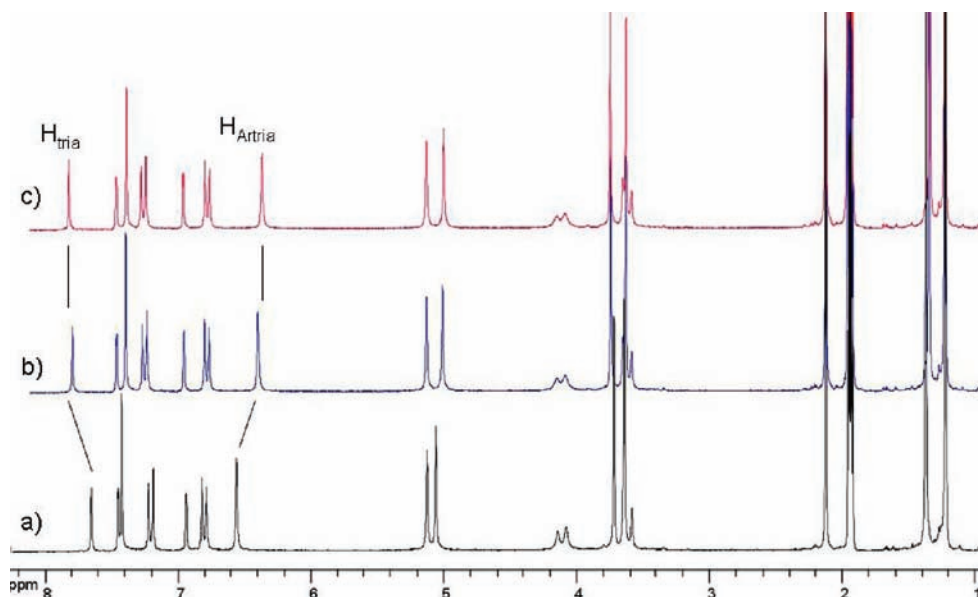


**Figure 3.**  $^1\text{H}$  NMR ( $\text{CD}_3\text{CN}$ , 300 K, 250 MHz) titration of  $[\text{Zn}^{\text{II}}_{\text{Im}}(\mathbf{1})(\text{CD}_3\text{CN})](\text{ClO}_4)_2$  with  $[\text{Cu}(\text{CH}_3\text{CN})_4](\text{PF}_6)$ : (a) 0, (b) 1, and (c) 1.5 equiv.

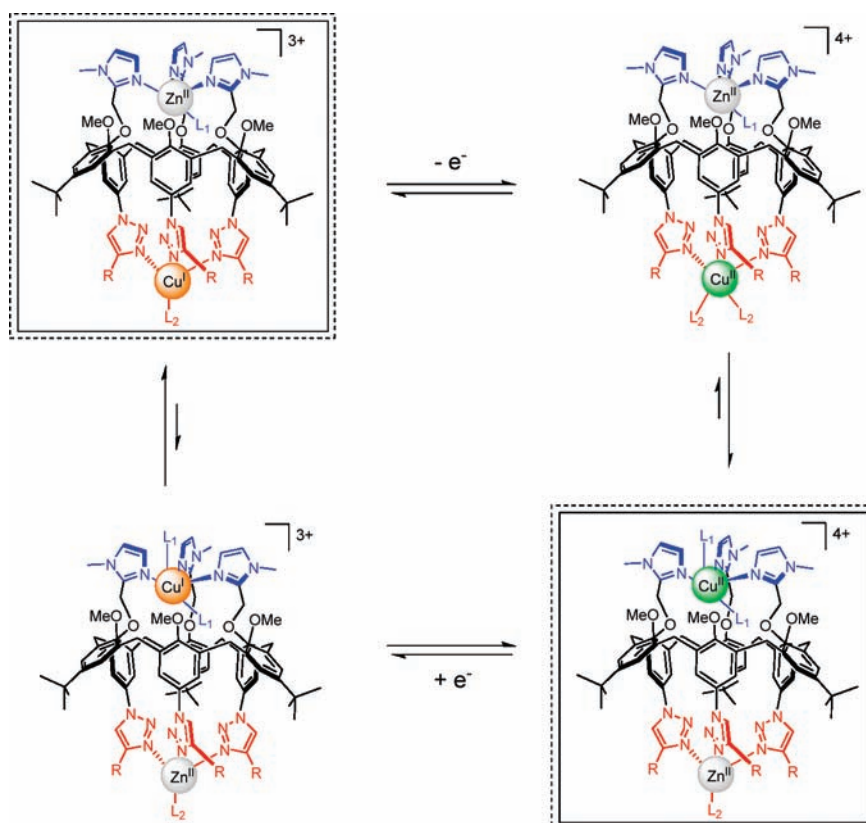
$[\text{Zn}^{\text{II}}_{\text{Im}}\text{Cu}^{\text{I}}_{\text{Tria}}(\mathbf{1})(\text{CH}_3\text{CN})]^{3+}$  (Figure S6, Supporting Information). Also, when CO was bubbled into a  $\text{CDCl}_3$  solution of the bimetallic complex, an IR stretch for CO was observed at  $2098\text{ cm}^{-1}$  with only small shifts for the NMR resonances of the protons  $\text{H}_{\text{Tria}}$  ( $\Delta\delta = 0.07\text{ ppm}$ ) (Figure S8, Supporting Information). The encapsulated  $\text{CH}_3\text{CN}$  molecule bound to  $\text{Zn}^{2+}$  was also shifted ( $\Delta\delta = -0.09\text{ ppm}$ ). All these data show that in the most stable situation for the  $\text{Zn}^{\text{II}}/\text{Cu}^{\text{I}}$  combination the  $\text{Zn}^{\text{II}}$  is located at the small rim site (Im) and the  $\text{Cu}^{\text{I}}$  at the large rim site (Tria). Both metal centers are in a tetrahedral environment with three positions being occupied by the *N*-Im or the *N*-Tria of  $\mathbf{1}$ , the fourth one being labile and accessible to an exogenous ligand molecule (for instance,  $\text{CH}_3\text{CN}$ ).

**$\text{Zn}^{\text{II}}/\text{Cu}^{\text{II}}$ .** Addition of 1 equiv of  $[\text{Cu}(\text{H}_2\text{O})_6](\text{ClO}_4)_2$  to a THF solution containing  $[\text{Zn}^{\text{II}}_{\text{Im}}(\mathbf{1})(\text{H}_2\text{O})](\text{ClO}_4)_2$  resulted in the precipitation of a green solid whose composition, checked by elemental analysis, is in good agreement with the formula  $[\text{Zn}^{\text{II}}\text{Cu}^{\text{II}}(\mathbf{1})(\text{H}_2\text{O})_3](\text{ClO}_4)_4$ . The spectroscopic data for this complex (Table 1 and Figures S11–S15, Supporting Information) are very similar to those of  $[\text{Cu}^{\text{II}}_{\text{Im}}(\mathbf{1})(\text{H}_2\text{O})_2](\text{ClO}_4)_2$ . We therefore concluded that the  $\text{Cu}^{\text{II}}$  cation is located at the Im site and the  $\text{Zn}^{\text{II}}$  at the Tria site. In order to confirm the coordination sites of this heterobimetallic complex, that is, to determine the regioisomerism of the coordination, we performed a UV–vis titration of a  $\text{CH}_3\text{CN}$  solution of  $[\text{Cu}^{\text{II}}_{\text{Im}}(\mathbf{1})(\text{H}_2\text{O})_2]^{2+}$  (1.7 mM) with  $\text{Zn}(\text{ClO}_4)_2 \cdot 6\text{H}_2\text{O}$  (Figure S9, Supporting Information). The intensity of the d–d band centered at 757 nm slightly increased until 1 equiv of  $\text{Zn}^{\text{II}}$  was added, after which it reached a plateau (Figure S10, Supporting Information). Moreover,  $\lambda_{\text{max}}$  remained almost unchanged (only a 2 nm shift) (Figure S11, Supporting Information). This emphasizes that after addition of 1 equiv of  $\text{Zn}^{\text{II}}$  the coordination sphere around the copper cation remained the same. Therefore,  $\text{Zn}^{\text{II}}$  coordinates the Tria site. It also indicates that a 1:1 adduct is yielded and that the final species present in solution is the  $[\text{Cu}^{\text{II}}_{\text{Im}}\text{Zn}^{\text{II}}_{\text{Tria}}(\mathbf{1})(\text{L})_3]^{4+}$  complex ( $\text{L} = \text{CH}_3\text{CN}$  or  $\text{H}_2\text{O}$ ).

**Double Translocation for the  $\text{Zn}^{\text{II}}/\text{Cu}^{\text{III}}$  Complexes.** While the two monometallic  $\text{Cu}^{\text{II}}$  and  $\text{Cu}^{\text{I}}$  complexes bind the cation at the Im site, the Im/Tria ditopic ligand adopts, in the presence of  $\text{Zn}^{\text{II}}$ , the two reverse binding modes for  $\text{Cu}^{\text{II}}$  and  $\text{Cu}^{\text{I}}$  at the

Im and the Tria sites, respectively. We then tested the possibility to trigger the translocation of the two Cu cations by an electrochemical input (Scheme 1). The redox behavior of  $[\text{Zn}^{\text{II}}_{\text{Im}}\text{Cu}^{\text{I}}_{\text{Tria}}(\mathbf{1})(\text{CH}_3\text{CN})_2](\text{PF}_6)(\text{ClO}_4)_2$  was investigated in the same medium at different concentrations ( $\leq 2\text{ mM}$ ). As shown in Figure 2B, oxidation of the  $[\text{Zn}^{\text{II}}_{\text{Im}}\text{Cu}^{\text{I}}_{\text{Tria}}(\mathbf{1})(\text{CH}_3\text{CN})_2]^{3+}$  complex occurs irreversibly at  $E_{\text{pa}} = 0.75\text{ V}$  when  $C = 2\text{ mM}$ . The reduction of the electrochemically generated oxidized product corresponds to an irreversible peak at  $E_{\text{pc}} = 0.01\text{ V}$  on the reverse scan (Table 1). No reversibility for both peaks could be obtained on the second scan and for all investigated scan rates ( $0.01 < \nu < 50\text{ V s}^{-1}$ ) at this concentration. Randles–Sevcik plots yield a linear dependence of the anodic peak intensity  $i_{\text{pa}}$  with the square root of the scan rate ( $\nu^{1/2}$ ), thus attesting to a diffusion-limited electron-transfer process (Figure S20, Supporting Information). RDEV showed the presence of only one species in solution which is oxidized at  $E_{1/2} = 0.70\text{ V}$  (Figure 4A, curve a). Quantitative electrolysis at 1 V yields a  $\text{Cu}^{\text{II}}$  species which is reduced at  $E_{1/2} \approx 0.00\text{ V}$  (Figure 4A, curve b). The CV of this complex shows an irreversible peak at  $E_{\text{pc}} = 0.00\text{ V}$  associated with an irreversible reoxidation peak at  $E_{\text{pa}} = 0.75\text{ V}$  (Figure 4B, curve a). Moreover, the EPR spectrum of the solution after electrolysis is almost identical to the chemically synthesized  $[\text{Cu}^{\text{II}}_{\text{Im}}\text{Zn}^{\text{II}}_{\text{Tria}}(\mathbf{1})(\text{H}_2\text{O})_3]^{4+}$  complex (Figure 5).

By comparison with the data for the mono-copper and bis-copper complexes (see above), the anodic peak at  $E_{\text{pa}} = 0.75\text{ V}$  is ascribed to the oxidation of a  $[\text{Zn}^{\text{II}}_{\text{Im}}\text{Cu}^{\text{I}}_{\text{Tria}}(\mathbf{1})(\text{CH}_3\text{CN})_2]^{3+}$  complex whereas the cathodic peak at 0.01 V corresponds to the reduction of a  $[\text{Cu}^{\text{II}}_{\text{Im}}\text{Zn}^{\text{II}}_{\text{Tria}}(\mathbf{1})(\text{L})_3]^{4+}$  ( $\text{L} = \text{CH}_3\text{CN}$  or  $\text{H}_2\text{O}$ ) species (Table 1). The same CV behavior is observed with the chemically synthesized  $\text{Zn}^{\text{II}}/\text{Cu}^{\text{II}}$  complex,  $[\text{Cu}^{\text{II}}_{\text{Im}}\text{Zn}^{\text{II}}_{\text{Tria}}(\mathbf{1})(\text{L})_3]^{4+}$ , which displays an irreversible reduction of the cupric ion being in the Im environment at  $E_{\text{pc}} = 0.01\text{ V}$ , with, on the reverse scan, an irreversible anodic peak at  $E_{\text{pa}} = 0.70\text{ V}$  (Figure 4B, curve b, and Figure S21, Supporting Information). Quantitative electrolysis at  $E = -0.20\text{ V}$  yielded back a species which behaves exactly as the  $[\text{Zn}^{\text{II}}_{\text{Im}}\text{Cu}^{\text{I}}_{\text{Tria}}(\mathbf{1})(\text{L})_2]^{3+}$  compound. This clearly establishes the reversible interconversion between the two stable species  $[\text{Zn}^{\text{II}}_{\text{Im}}\text{Cu}^{\text{I}}_{\text{Tria}}(\mathbf{1})(\text{L})_2]^{3+}$  and  $[\text{Cu}^{\text{II}}_{\text{Im}}\text{Zn}^{\text{II}}_{\text{Tria}}(\mathbf{1})(\text{L})_3]^{4+}$ . Hence, the CV

**Scheme 1.** Schematic Representation of the Double Translocation Process in  $\text{CH}_3\text{CN}^a$ 

<sup>a</sup> Stable complexes are depicted in rectangles.

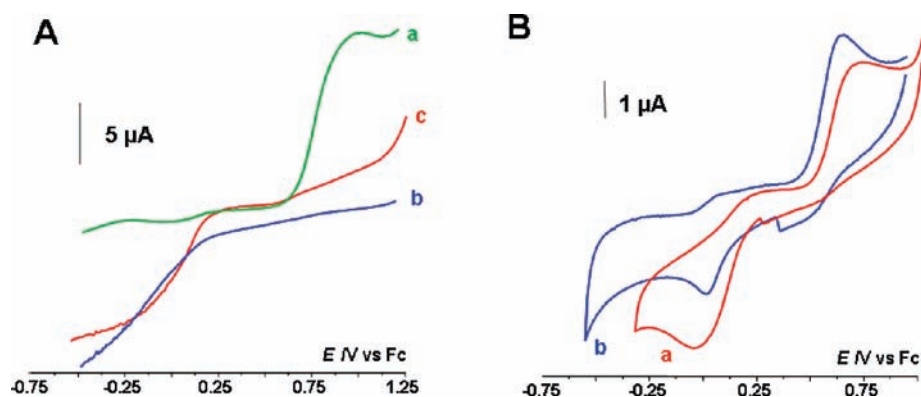


**Figure 4.** (A) RDE voltammogram ( $\omega = 1500$  t/min) at a Pt electrode ( $E/V$  vs Fc) in 0.1 M  $\text{CH}_3\text{CN}/\text{NBu}_4\text{PF}_6$  of  $[\text{Zn}^{\text{II}}_{\text{Im}}\text{Cu}^{\text{I}}_{\text{Tria}}(\mathbf{1})(\text{CH}_3\text{CN})_2](\text{ClO}_4)_2(\text{PF}_6)$ , concentration = 2 mM (a) before and (b) after electrolysis at 1.00 V; (c) RDEV of  $[\text{Cu}^{\text{II}}_{\text{Im}}\text{Zn}^{\text{II}}_{\text{Tria}}(\mathbf{1})(\text{H}_2\text{O})_3](\text{ClO}_4)_4$ . (B) Cyclic voltammogram ( $\nu = 0.1$   $\text{V}\cdot\text{s}^{-1}$ ) at a Pt electrode ( $E/V$  vs Fc) in 0.1 M  $\text{CH}_3\text{CN}/\text{NBu}_4\text{PF}_6$  of (a)  $[\text{Zn}^{\text{II}}_{\text{Im}}\text{Cu}^{\text{I}}_{\text{Tria}}(\mathbf{1})(\text{CH}_3\text{CN})_2](\text{ClO}_4)_2(\text{PF}_6)$  after bulk electrolysis at 1.00 V and (b)  $[\text{Cu}^{\text{II}}_{\text{Im}}\text{Zn}^{\text{II}}_{\text{Tria}}(\mathbf{1})(\text{H}_2\text{O})_3](\text{ClO}_4)_4$ .

behavior can be identified as two successive electrochemical–chemical (EC) processes, corresponding to a classical square scheme (Scheme 1). The electrochemical step (E, Cu oxidation or reduction) is followed by the fast (vs the time scale of the experiment) concomitant motions of the Cu and  $\text{Zn}^{\text{II}}$  ions from one site to the other (which corresponds to a global chemical step C). It thus can be considered that, at the time scale of the CV, the electron transfer induces a heteronuclear reversible double translocation both in oxidation and in reduction.<sup>12b</sup> A CV simulation allowed reproducing the general trends of the CV curves at different scan rates for the  $[\text{Zn}^{\text{II}}_{\text{Im}}\text{Cu}^{\text{I}}_{\text{Tria}}(\mathbf{1})(\text{L}_2)]^{3+}$  complex on the basis of the square scheme presented in Scheme 1 (see the Supporting Information for simulated voltammograms).

Interestingly, voltammetric studies performed at lower concentrations (ca 0.1 mM) resulted in a different behavior with the appearance of reversibility for both systems (Table 1) (Figure S22, Supporting Information). This suggests that the double translocation processes involve a bimolecular step, which is rate determining. Oxidation of the stable  $\text{Zn}^{\text{II}}_{\text{Im}}/\text{Cu}^{\text{I}}_{\text{Tria}}$  species into  $\text{Zn}^{\text{II}}_{\text{Im}}/\text{Cu}^{\text{II}}_{\text{Tria}}$  labilizes the  $\text{Cu}^{\text{II}}$  ion due to its poor affinity for the Tria site, a weak donor, and a trigonal enforcer, which can undergo fast decoordination/recoordination. Likewise, reduction of the stable  $\text{Cu}^{\text{II}}_{\text{Im}}/\text{Zn}^{\text{II}}_{\text{Tria}}$  species produces the more labile  $\text{Cu}^{\text{I}}$  ion, a poor structuring agent, which then can also undergo fast decoordination/recoordination. Hence, a possible mechanism for the translocation may first involve the release of a labilized

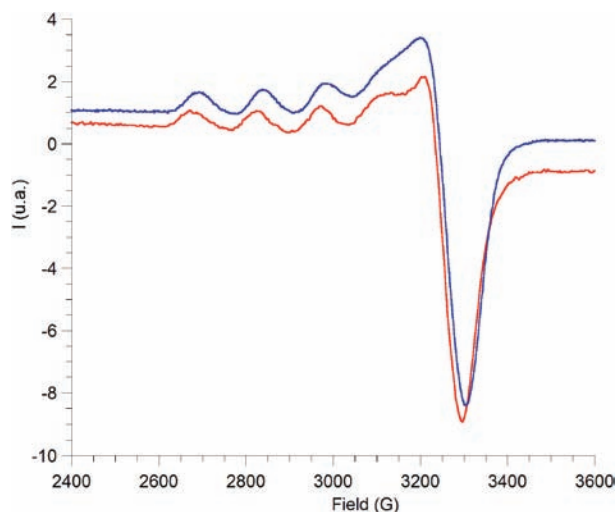


**Figure 5.** EPR spectra (0.1 M  $\text{CH}_3\text{CN}/\text{NBu}_4\text{PF}_6$ , 150 K) of  $[\text{Cu}^{\text{II}}_{\text{Im}}\text{Zn}^{\text{II}}_{\text{Tria}}(\mathbf{1})(\text{H}_2\text{O})_3](\text{ClO}_4)_4$  (blue) and the product obtained by electrolysis of  $[\text{Zn}^{\text{II}}_{\text{Im}}\text{Cu}^{\text{I}}_{\text{Tria}}(\mathbf{1})(\text{CH}_3\text{CN})_2](\text{ClO}_4)_2(\text{PF}_6)$  (red).

copper ion followed by its recoordination (a bimolecular process), which is a slow step when it is associated to the shift of  $\text{Zn}^{\text{II}}$  (either intermolecular or intramolecular<sup>14</sup>), to produce the most thermodynamically stable species.

## Conclusion

The electrochemically controlled motion of two different cations within a molecular complex has been achieved. The ditopic calixarene ligand studied in this work is able to bind differently the couple Zn/Cu depending on the oxidation state of copper. This new double translocation, which is electrochemically monitored, can be observed because several features are combined in ligand **1**: (i) in a monometallic complex, the cation is preferentially coordinated at the more donating Im site; (ii) this Im site is geometrically flexible and can accommodate a trigonal or tetragonal coordination sphere around a metal center; (iii) coordination of a cation at the Im site rigidifies the whole structure and prevents the Tria site from coordinating a tetragonal cation like  $\text{Cu}^{\text{II}}$ . The  $\text{Zn}^{\text{II}}$  cation is thus essential to give the system its bistability. Indeed, in the absence of the allosteric effect of the  $\text{Zn}^{\text{II}}$ , the ligand binds both  $\text{Cu}^{\text{I}}$  and  $\text{Cu}^{\text{II}}$  preferentially in the same trisimidazole environment. The mechanism, which corresponds formally to a bis-translocation, is not yet fully understood, but our first experimental evidence supports an intermolecular pathway.

(14) The motion of a cation in a ditopic calixarene platform has already been observed (“molecular syringe” for  $\text{Ag}^+$  under acid–base stimulus). Ikeda, A.; Tsudera, T.; Shinkai, S. *J. Org. Chem.* **1997**, *62*, 3568–3574.

This study has revealed a possible way to trigger the translocation of two different metal ions by a redox process associated to allosteric control. Interesting parallels with biological processes can be drawn for each aspect: on one hand, allosteric control by  $\text{Zn}^{\text{II}}$  has been evidenced for the copper loading in the enzyme (Zn,Cu)-superoxide dismutase;<sup>15</sup> on the other hand, a redox-triggered translocation of a copper ion from one side of a protein to another has been recently described, thus suggesting a possible general pathway for copper trafficking in living organisms.<sup>16</sup> From an applicative point of view, our system can also be envisioned as a proof of concept for the possible elaboration of a bistable device where a structuring metal ion (here  $\text{Zn}^{\text{II}}$ ) allows the redox-triggered translocation of another one ( $\text{Cu}^{\text{II}}/\text{Cu}^{\text{I}}$ ).<sup>17</sup>

## Experimental Section

General procedures, synthesis, and characterization of the complexes, UV–vis, EPR, and  $^1\text{H}$  NMR spectra, are given in the Supporting Information. The electrochemical studies of the copper complexes have been performed in a glovebox (Jacomex) ( $\text{O}_2 < 1$  ppm,  $\text{H}_2\text{O} < 1$  ppm) with a home-designed 3-electrode cell (WE, Pt; RE, Pt in  $\text{Fc}^+/\text{Fc}$  solution; CE, Pt). The potential of the cell was controlled by an AUTOLAB PGSTAT 100 (Ecochemie) potentiostat monitored by a computer. Anhydrous “extra-dry” dichloromethane ( $\text{H}_2\text{O} < 30$  ppm, Acros) and acetonitrile (99.9% BDH, VWR) were used as received and kept under  $\text{N}_2$  in the glovebox. The supporting salt  $\text{NBu}_4\text{PF}_6$  was synthesized from  $\text{NBu}_4\text{OH}$  (Fluka) and  $\text{HPF}_6$  (Aldrich). It was then purified, dried under vacuum for 48 h at 100 °C, and kept under  $\text{N}_2$  in the glovebox. The electrolyte  $\text{NBu}_4\text{ClO}_4$  (99.0%, Sigma-Aldrich) was used as received. UV–vis–NIR spectroscopy was performed with a JASCO V-670 spectrophotometer. EPR spectra were recorded on a Bruker ELEXSYS E500 apparatus.

**Acknowledgment.** This research was supported by CNRS and Agence National pour la Recherche (Calixzyme Project ANR-05-BLAN-0003).

**Supporting Information Available:** General procedures, synthesis, and characterization of the complexes, spectroscopic data (UV–vis, EPR, and  $^1\text{H}$  NMR), electrochemical experiments, and simulation. This material is available free of charge via the Internet at <http://pubs.acs.org>.

JA910676Z

- (15) It has been shown that the  $\text{Zn}^{\text{II}}$  cation has a key role for copper loading in Zn, Cu–superoxide dismutase (SOD) as the copper chaperon CCS transfers its copper ion only to the Zn-metallated SOD protein and not to the apoprotein. Banci, L.; Bertini, I.; Cramaro, F.; Del Conte, R.; Viezzoli, M. S. *Biochemistry* **2003**, *42*, 9543–9553.
- (16) Arnesano, F.; Banci, L.; Bertini, I.; Mangani, S.; Thompson, A. R. *Proc. Natl. Acad. Sci. U.S.A.* **2003**, *100*, 3814–3819.
- (17) (a) Balzani, V.; Credi, A.; Venturi, M. *Molecular Devices and Machines—A Journey into the Nanoworld*; Wiley-VCH: Weinheim, 2003. (b) Champin, B.; Mobian, P.; Sauvage, J.-P. *Chem Soc. Rev.* **2007**, *36*, 358–366.